Green synthesise of CuO@Fe_3O_4@Xantan nanocomposites and its application in enhanced oil recovery by considering IFT and wettability behaviours

Abbas Khaksar Manshad[1] ✉, *Jagar A. Ali*[2,3], *Irfan Imani*[1], *S. Mohammad Sajadi*[4,5], *Nabil A. Tayeb Ubaid*[6], *Alireza Keshavarz*[7]

[1]*Department of Petroleum Engineering, Abadan Faculty of Petroleum Engineering, Petroleum University of Technology (PUT), Abadan, Iran*
[2]*Department of Petroleum Engineering, Faculty of Engineering, Soran University, Soran, Kurdistan Region, Iraq*
[3]*Department of Petroleum Engineering, College of Engineering, The American University of Kurdistan, Duhok, Kurdistan Region, Iraq*
[4]*Department of Nutrition, Cihan University-Erbil, Kurdistan Region, Iraq*
[5]*Scientific Research Center, Soran University, P.O. Box 624, Soran, Kurdistan Regional Government, Iraq*
[6]*Petroleum and Energy Engineering Department, Sulaimani Polytechnic University, Sulaymaniyah, Kurdistan Region, Iraq*
[7]*School of Engineering, Edith Cowan University, WA 6027, Australia*
✉ *E-mail: akmanshad113@gmail.com*

Published in Micro & Nano Letters; Received on 15th July 2019; Revised on 24th March 2020; Accepted on 9th April 2020

Enhanced oil recovery (EOR) makes use of various chemical processes to extract additional oil from reservoirs, often already under production. In this study, authors investigated the role of the CuO@Fe_3O_4@xanthan nanocomposite (NCs) in EOR by the focus of the interfacial tension (IFT) and wettability alteration mechanisms. This NCs is synthesized from *Artocarpus altilis* extract using a simple, economical and green method. The prepared NCs is identified using X-ray diffraction (XRD), Fourier-transform infrared spectroscopy (FTIR), and scanning electron microscopy (SEM). Nanofluids are prepared from dispersing the synthesised NCs in water at different concentrations in order to be used in the density, viscosity, conductivity, IFT and contact angle measurements. The results showed an improvement in the values of IFT and contact angle. The IFT of oil/water is increased from 22 to 24 mN/m with increasing the concentration of the NCs from 250 to 2000 ppm. While, the wettability of the carbonate rock is remained water-wet, wherein the contact angle is raised from 28° to 58° with increasing the NCs concetration from 250 to 2000 ppm. Overall, the IFT and contact angle are only reduced when 250 ppm NCs was added to water from 28.3 mN/m and 132.6° mN/m to 22 and 34.5°.

1. Introduction: The world demand for oil a key source of energy continues to be increased in recent years and the primary oil production is unable to supply this demand any further [1–4]. Discovering new oilfields become difficult and the oil production from the mature reservoirs is declining [5]. Thus, improving the recovery from the current-producible reservoirs has been more concentrated by the researchers and the industry [6]. Water flooding, as a common secondary recovery process, was mostly applied to maintain the internal forces and drive mechanisms of oil reservoirs after the depletion phase [7]. However, several considerable difficulties are experienced frequently during the flooding process, specifically in carbonate reservoirs, for example, the oil bypass and trapping due to the poor sweep and displacement efficiencies of the injected water. The interfacial tension (IFT) and rock wettability between the present fluids are the main parameters that affect the recovery efficiency are proven to be crucial factors [8–10]. Chemical processes were conventionally used to alter the wettability of the rocks toward water-wet conditions and reduce the IFT between oil and aqueous phases [11, 12]. Nonetheless, the high cost of such materials, the possibility of reservoir damage, loss through chemical activity are the main challenges when applying the current enhanced oil recovery (EOR) methods [10, 11]. Indeed, new EOR technology with low cost, high efficiency, and which is eco-friendly needs to be developed. Based on this principle, recently, nanoparticles (NPs) in solution form as nanofluids have received significant attention for EOR applications. Such innovative fluids are developed by mixing NPs with various base fluids, like brine, polymeric solutions, glycols, and alcohols. Nanofluids can improve the rock-fluid and/or fluid-fluid interactions that reduce IFT, changes wettability, and ultimately improve sweep efficiency [12–15]. NPs have been reported to be stable agents for EOR due to their small particle size, high surface area, and dispersion stability [16]. Various NPs were used for increasing oil recoveries, such as silicon dioxide (SiO_2), titanium dioxide (TiO_2), aluminium oxide (Al_2O_3), iron(III) oxide (Fe_2O_3), copper oxide (CuO), zinc oxide (ZnO), and nickel oxide (NiO).

The efficiency and functions of NPs can be improved by modifying the surface of NPs. Ju and Fan [17] prepared and used the polymer-coated SiO_2 to alter the rock wettability and reduce IFT, and they were enabled to increase oil recovery by up to 21%. Rezvani *et al.* [18] were successful in producing 10.8% original oil in place (OOIP) an extra oil by using Fe_3O_4/chitosan nanocomposite (NC) due to modifying the IFT and wettability behaviours. Also, Qi *et al.* [19] could increase the residual oil recovery by 10% from coating the surface of the silica NPs by a polymer. However, Lim and Wasan [20] dispersed CuO in polyethylene glycol and were not successful in producing an extra crude oil compared to the water-based nanofluid flooding. Meanwhile, Zhang *et al.* [13] dispersed SiO_2 in polyethylene glycol, and they enabled to produce more oil recovery ranged 17% by the combined effect of IFT reduction and wettability alteration.

Ali *et al.* [21] obtained a huge reduction in IFT (93%), significant alteration in wettability towards a water-wet system and high improvement in oil recovery (19.3%) from using a green-synthesised ZnO/SiO_2/Xanthan NC due to creating better interactions between crude oil – polymer – NPs – carbonate rocks. Afterwards, we synthesised some more green NCs for the petroleum and EOR applications [22–24]. In addition, several researchers synthesised iron NPs using a green method from the plant extract, such as Madhavi *et al.* [25] used the leaf extracts of *Eucalyptus globules*, Kuang *et al.* [26] used the tea extract, Muthukumar and Matheswaran [27] used the extract of the

doi: 10.1049/mnl.2019.0431

Amaranthus spinosus leaf, Sajadi *et al.* [28] used the aqueous extract from seeds of *Silybum marianum*, Groiss *et al.* [29] used the leaf extract of *Cynometra ramiflora* plant, Sajadi *et al.* [30] used the *Euphorbia peplus Linn* leaf, and the extract of *Eichhornia crassipes* used by Wei *et al.* [31]. In this study, we fabricated a composite nanomaterial from depositing the copper and magnetite NPs on the surface of the Xanthan gum polymer. We used a simple and green method to synthesis the NPs and then NCs from the extract of the *Artocarpus altilis* plant. Instead of having NPs dispersed in the polymer, we prepared the polymeric-nanofluid by dispersing the synthesised CuO@Fe_3O_4@Xanthan NCs in seawater under various salinity conditions. The developed nanofluids were used in the IFT and contact angle measurements. *Artocarpus altilis* is a species of flowering tree from the family of *Moraceae* and native to Melanesia, which widely distributed throughout the South Pacific and other tropical areas. The plant has some biological properties such as haemolytic, antibacterial and antitumour activities. Among the various bioactive phytochemicals of the plant proteins, different types of vitamins, especially vitamin C, flavonoids and glycosides, are considerable [32–35]. Therefore, the presence of phenolic such as flavonoids aglycones and their glycosides and also vitamin C as known antioxidant compounds caused to the application of the plant as bioreducers and stabilising agents for green synthesis of nanostructures. Also, the application of Xanthan here is as the natural substrate for increasing the surface area of NC, increasing the number of active sites per unit area of the catalyst, increasing the stability of the NC and finally preventing the agglomeration and aggregation side effects.

2. Materials and methods

2.1. Materials: High-purity chemical reagents including Iron(II) chloride ($FeCl_2$), Iron(III) chloride ($FeCl_3$), Copper(II) Chloride Dihydrate ($CuCl_2{\cdot}_2H_2O$), methanol, n-hexane and ethanol were purchased from the Merck company with a purity higher than 99 mol%. Crude oil of a density of 0.879 g/cc (29.5° API) was taken from the Asmari reservoir of the Rag-e-sefid Oilfield in Iran, which was filtered with a 5 µm mesh. The number of aromatic compounds is the highest at 37%, and asphaltene products showed a minimum percentage of 10%. While the percentage of saturate and resin compounds are 29 and 24, respectively. A carbonate rock was collected from the Asmari Outcrop in southwest Iran for contact angle measurements.

2.2. Phytosynthesis of CuO@magnetite@Xanthan NC and its characterisation: The detailed steps of the experimental procedure of synthesising CuO@magnetite@Xanthan NCs were schematically illustrated in Fig. 1. Firstly, the plant extract was prepared by mixing 50 g of dried powder of the *Artocarpus altilis* leaves with 500 ml distilled water at 80°C for 30 min under reflux conditions. Then, the obtained aqueous extract was filtered and stored at 4°C. In a 250 ml conical flask, 1.5 g $FeCl_2$ and 3 g $FeCl_3$ were mixed with 100 ml *Artocarpus altilis* extract containing 0.6 gm $CuCl_2{\cdot}_2H_2O$ while stirring at 80°C for 5 h. Afterwards, the obtained precipitation was separated and refluxed with an ethanolic suspension of Xanthan gum (10 gm) for an extra 5 h. Finally, the completely mixed solution was dried was dried and kept for further investigations. Moreover, the scanning electron microscope (SEM) technique was used to characterise the size and shape of Fe_3O_4@Mineral-soil NC. Additionally, X-ray diffraction (XRD, Philips powder diffractometer type PW 1373, Goniometer-Cu $K\alpha = 1.5406$ Å) and Fourier transform infrared spectroscopy (FTIR) analytical approaches were used to study the mineralogical composition of prepared nanomaterial. Beside the amorphous system of Xanthan as a natural substrate which caused to show no crystalline signal in the XRD pattern, but this pattern shows a crystalline system for green synthesised NPs but as the amount of substrate is more considerable in contrast with the CuO and magnetite NPs, this is overlapping for their signals.

Furthermore, the FTIR spectrum of green synthesised NCs shows some signals at 3433, 2921, 1732, 1616 and 1418, 1000–1350 and 888 cm^{-1}, which are assigned to the OH and Fe–O stretching, C–H-SP3, C=O, C=C, C–O and Fe–O bending bonds. The presence of these functional groups shows the adsorption of phytochemicals on the surface of NCs.

2.3. Preparation and characterisation of nanofluids: To prepare the nanofluids, distilled water was used as the continues aqueous phase. The synthesised CuO@magnetite@Xanthan NCs were dispersed in distilled water at different concentrations of 250, 500, 1000, 1500 and 2000 ppm. These nanofluids were prepared using stirring (LABINCO L81 Stirrer) at 600 rpm for 6 h with keeping the operating temperature below 30°C. Additionally, to keep NCs dispersed within the distilled water, nanofluids were mixed using ultrasonic waves emitted from the UIP 200HD ultrasonic mixer, manufactured by Hielscher in Germany, for 2 h. Nanofluids characteristics of including density, conductivity and pH at ambient temperature and pressure conditions were measured using PAAR density meter, Mettler Toledo S230, and WTW™ inoLab™ Cond 7310, respectively.

2.4. Interfacial tension measurement: In this study, the pendant drop method was used to measure interfacial tension of liquid–liquid system using an IFT-400 apparatus from estimating the dimensions of the suspended crude oil droplet (Fig. 2). After receiving the droplet image in the computer from a camera, the software will start to identify the value of IFT using equation

$$\gamma = \frac{\Delta\rho \cdot g \cdot D}{H} \tag{1}$$

where $\Delta\rho$ is the difference between the density of the drop and bulk fluids (gm/cm^3), g is the gravitational acceleration of the earth (cm/s^2), D is the large diameter of the droplet (cm), and H is the droplet shape factor. IFT between crude oil and nanofluids (NF250, NF500, NF1000 and NF1500) with different concentrations of CuO@magnetite@Xanthan NCs was measured.

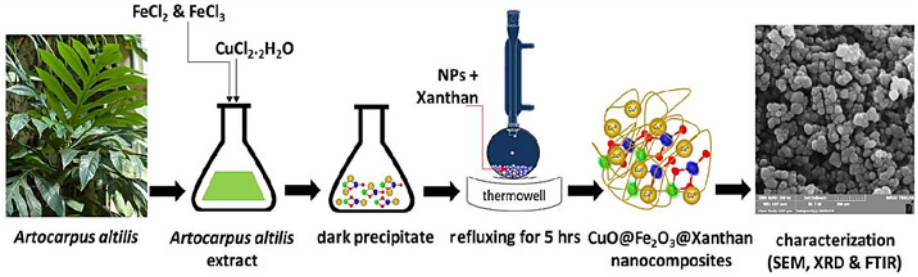

Fig. 1 *Schematic diagram of the biosynthesis process for preparing green CuO@magnetite@Xanthan NCs*

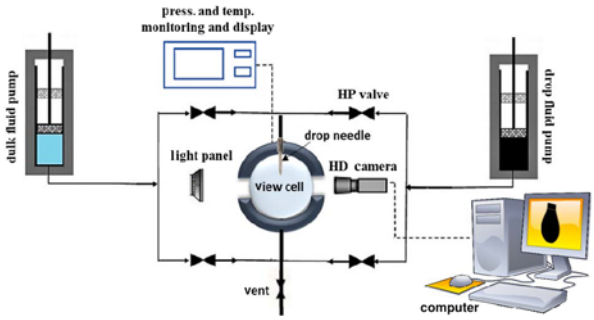

Fig. 2 *Schematic presentation of high-pressure (HP) and high-temperature (HT) pendant drop IFT400 measuring apparatus*

2.5. Contact angle measurement: In this study, the sessile drop technique was used to measure the contact angle between crude oil and various water-based nanofluids with different NC concentrations on the surface of the carbonate rocks (Fig. 3). Smooth pellets of carbonate rock were prepared from cutting the rock plugs into thin sections in 2 mm, and carefully polished and cleaned by distilled water and toluene to remove all the possible surface impurities. In addition, the trimmed carbonate pellets were aged by immersing and leaving inside the crude oil at a temperature of 70°C for 8 days. The contact angle of the crude oil droplet on carbonate rocks was estimated under the static condition submerging the prepared rock slices in enclosed containers filled with nanofluid solutions for 48 h.

3. Results and discussion

3.1. Characterisation of NC: The green CuO@magnetite@Xanthan NC was synthesised using the aqueous extract of *A. altilis* through an eco-friendly, fast and simple procedure. The main factor leading to this biosynthesis was the antioxidant potential of plant extract, which acts as bioredusing, stabilising and capping agents to increasing the synergistic effect of the green NC (Fig. 4). The magnetic effect of NC caused to its simple separation from the reaction media and its high recycling. After separation of the green NCs, it was elucidated using spectroscopic and micrograph techniques such as FTIR, XRD and SEM analytical techniques.

The crystallinity of green synthesised NCs was depicted by the XRD pattern in Fig. 5. Although the Xanthan substrate used to synthesis of green CuO@magnetite@Xanthan NC is amorph. Therefore it has no special signals in XRD diffractogram, but the characteristic peaks of the crystal planes, including crystalline minerals of CuO and Fe_3O_4 NPs are clearly depicted in the pattern. Moreover, to investigate the adsorption of phytochemicals on the surface of green synthesised NC, the FTIR spectrum of the green CuO@magnetite@Xanthan NC was assessed. According Fig. 6, signals around 3433, 1616, 1418 cm^{-1} and 1264–1000 cm^{-1} are assigned to the OH, C=O, C-sp2 of aromatics and C–C stretching vibrations. These functional groups are confidently belonging to the adsorbed phytochemicals on the surface of the green synthesised nanocatalyst which act as the

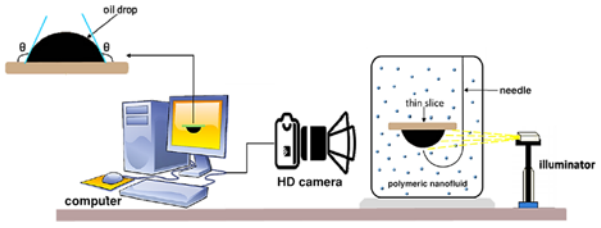

Fig. 3 *Schematic illustration of the sessile drop method for contact angle measurements [21]*

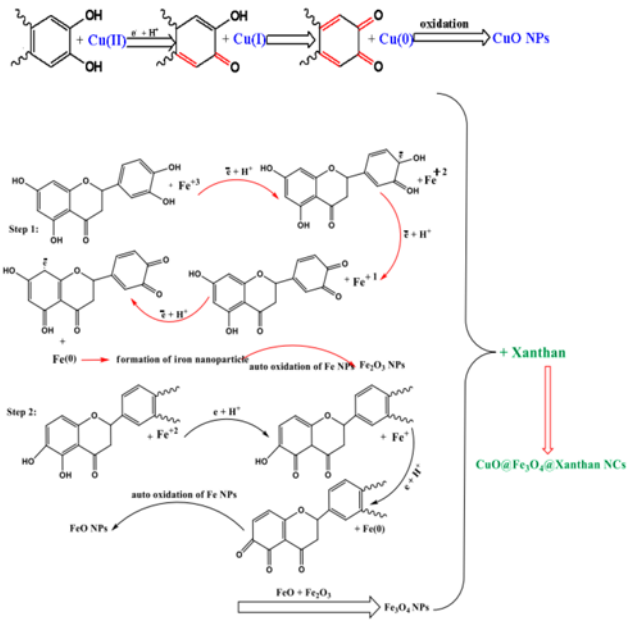

Fig. 4 *Mechanistic relationship of the synthesised NCs*

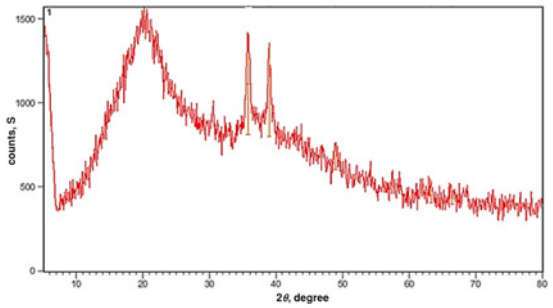

Fig. 5 *XRD pattern of the green synthesised NCs*

stabilising and capping agents and enhance the synergic effect and catalytic activity of NCs.

Furthermore, the surface morphology of the biosynthesised NCs was investigated with TEM and FE-SEM micrograph analysis, as depicted in Figs. 7 and 8. TEM results show the shape and nanoscale of the synthesised NCs, which is below 100 nm. As Fig. 8 shows, beside the presence of some agglomerations, the spherical and homogenous morphology of NPs deposited on the surface of Xanthan with the range size mostly between 40 and 70 nm is considerable. Therefore, according to these micrographs, the fabrication of NCs and its nanosized morphology is simply confirmed.

3.2. Characterisation of nanofluids: In this section, some main characteristics of the prepared nanofluids are presented and

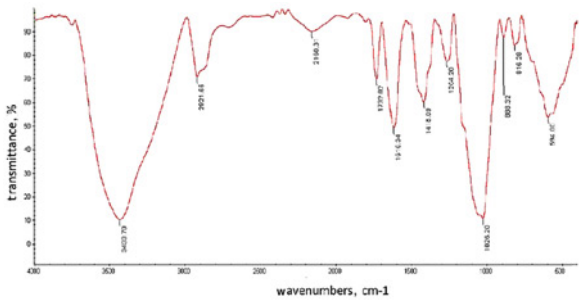

Fig. 6 *FTIR spectra of the green synthesised NCs*

doi: 10.1049/mnl.2019.0431

discussed, such as dispersion pH and conductivity. According to Fovet *et al.* [36] and Wen *et al.* [37], the pH of a colloidal solution significantly influences the particle aggregation and the stability of the suspension of the NPs, and having pH ranging between 6 and 7 is a good indication of high stability solution. Fig. 9*a* shows the pH values of the nanofluids, wherein the pH was reduced from 7.04 to 6.73 by adding 2000 ppm of synthesised NCs. The highest reduction in the value of pH was noticed when the concentration of NCs was increased from 500 to 1000 ppm, which was 80% of the total pH reduction. Then the pH was reduced slightly further from 6.87 to 6.81 and 6.73 when the NCs concentration increased to 1500 and 2000 ppm, respectively. Meanwhile, the conductivity readings of the prepared nanofluids formed by dispersing the synthesised NC in the diluted seawater are shown in Fig. 9*b*. As it can be seen that the conductivity was increased with increasing the NCs concentration. A conductivity of 61 µS/cm was measured for a nanofluid with 250 ppm of NCs and increased up to 199 µS/cm when the concentration of NCs increased to 2000 ppm.

3.3. IFT behaviour: Interfacial tension is one of the major EOR mechanisms that directly affect the capillary pressure in the porous media. According to Kamal *et al.* [38], increasing the capillary numbers from 10^{-7} and 10^{-6} to about 10^{-3} and 10^{-2} will reduce the oil saturation by 90% and to zero. To reach these values of saturation, IFT between oil and water must be reduced to its minimum value, which can be achieved by injecting chemical or nanofluid solutions. In this study, the IFT between crude oil and different nanofluids (NF250, NF500, NF1000, NF1500 and NF2000) was measured at ambient temperature and pressure (Fig. 10). The value of IFT decreased from 28.5 to 22 mN/m by adding 250 ppm of the synthesised NCs to the distilled water, which is considered as the minimum IFT obtained in this study. Then, IFT was increased with increasing the concentration of NCs to 500, 1000, 1500 and 2000 ppm; this is quite consistent with Eshraghi *et al.* [39], and Ali *et al.* [40, 41], where they only enabled to reduce the IFT to the optimum concentration of SiO_2 and then increased again with increasing the NPs concentration. The maximum IFT was measured between crude oil and NF2000 with 2000 ppm of $CuO@Fe_3O_4@$Xanthan NCs is 24 mN/m. Although there are no clear reasons behind the increase that happened in the IFT value with increasing the NCs concentration, the synthesised NCs did not show a great performance in terms of IFT reduction. Accordingly, 250 ppm can be considered as the optimum concentration of the used NCs, which resulted in the lowest IFT. For more clarification, shapes of crude oil droplets within the prepared nanofluid solutions (NF250, NF500, NF1000, NF1500 and NF2000) are illustrated in Fig. 11.

3.4. Wettability alteration: Wettability behaviour was estimated by measuring the contact angle of the crude oil droplet on the surface of the carbonate pellets within several nanofluid solutions (NF250, NF500, NF1000, NF1500 and NF2000). Fig. 12 illustrates the measured values of contact angles of the various aqueous systems. Initially, the contact angle of the system was measured without the presence of the synthesised NCs, which was 134° that indicates a strong oil-wet system [42–47]. Afterwards, the effect of the synthesised NCs on the wettability alteration was investigated by measuring the contact angle of different crude oil/nanofluids systems. Contact angles after nanofluid treatment were significantly reduced depending on the NCs concentrations. For this type of the aqueous phase, the lowest contact angle of 27.5° was measured for a crude oil treated with NF1000 nanofluid. However, the contact angle was increased 34° and 61° with increasing the concentration of NCs from 1500 and 2000 ppm, respectively. Generally, an intermediate to strong water-wet systems was observed for all nanofluid solutions at all different concentrations of $CuO@Fe_3O_4@$Xanthan NCs. While a strong water-wet condition was obtained at 1000 ppm NCs, which can be considered as

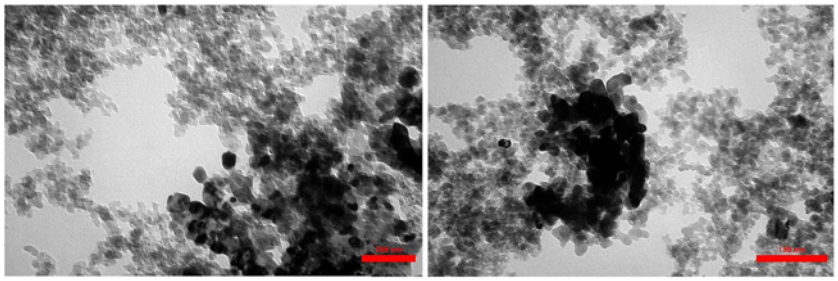

Fig. 7 *TEM images of the synthesised NCs at 100 and 150 nm*

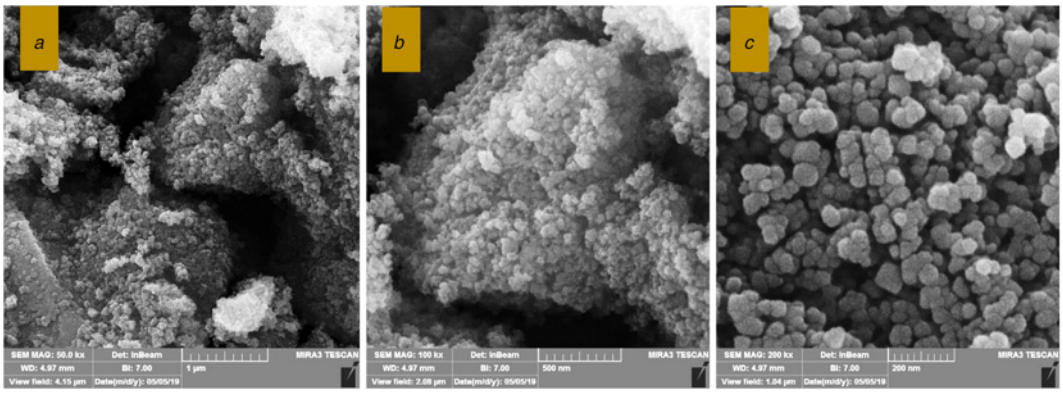

Fig. 8 *SEM morphologies CuO@magnetite@Xanthan NCs at*
a 1 µm and 50,000 × magnification
b 500 nm and 1,000,000 × magnification, and
c 200 nm and 200,000 × magnification

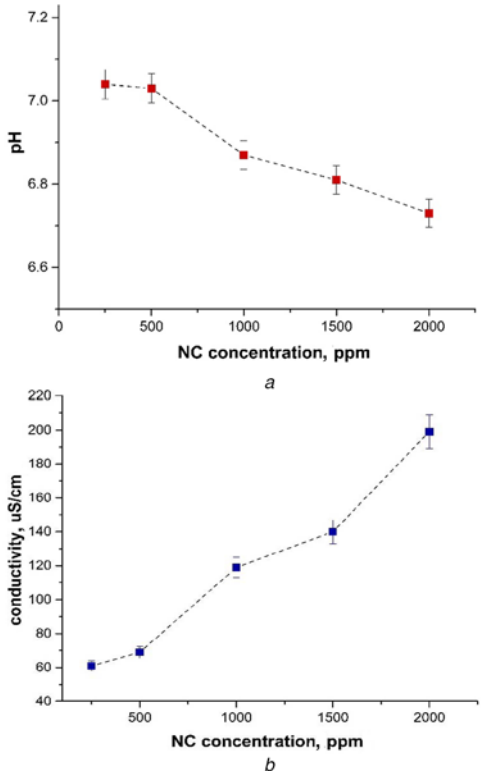

Fig. 9 *Characteristics of nanofluids with 250, 500, 1000, 1500 and 2000 ppm NCs concentrations*
a pH, and
b Conductivity

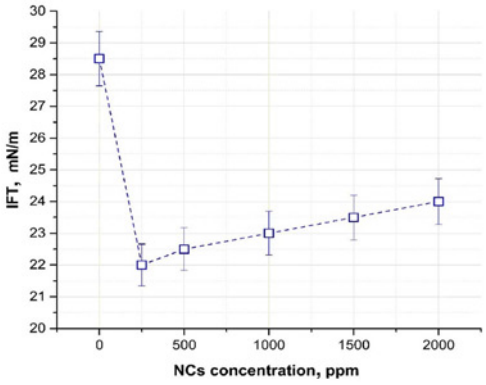

Fig. 10 *IFT values measured between crude oil and prepared nanofluids at different concentrations of CuO@Fe_3O_4@Xanthan NCs*

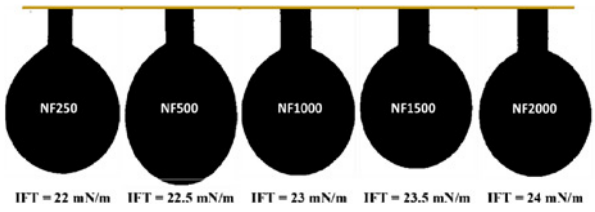

Fig. 11 *Shape profiles of crude oil droplets against the nanofluid solutions at different concentrations of CuO@Fe_3O_4@Xanthan NCs*

the optimal concentration of the NCs. This happened mainly due to the disjoining pressure of the nanomaterials when they tend to make a wedging force in an interface between the oil droplets and the carbonate surface. Moreover, to better understand the influences of the NCs concertation on the wettability alteration, contact angles of a

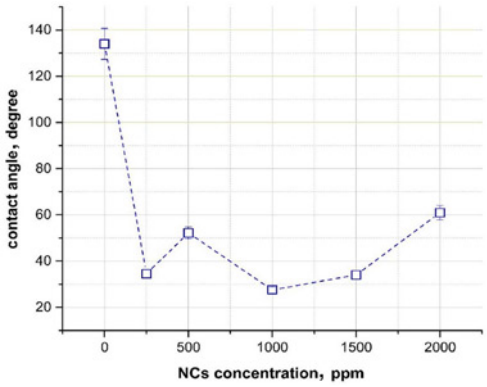

Fig. 12 *Measured contact angles the crude oil droplets on the surface of carbonate palettes with the presence of nanofluids at different concentrations of CuO@Fe_3O_4@Xanthan NCs*

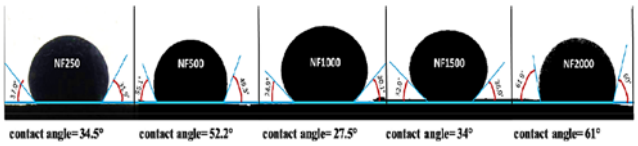

Fig. 13 *Shapes of crude oil droplets within NF250, NF500, NF1000, NF1500 and NF2000 nanofluids*

crude oil droplet on several carbonate slices aged NF250, NF500, NF1000, NF1500 and NF2000 were illustrated schematically in Fig. 13.

4. Conclusion: In this work, an objective-oriented NC, called CuO@Fe_3O_4@Xanthan, was synthesised for enhancing the recovery of oil from the mature oil reservoirs. The synthesised NC was composed of magnetite and copper NPs, which were synthesised from the extract of the *Artocarpus altilis* plant in green and economical way, and the Xanthan polymer. The production of these NCs was confirmed by conducting several characterisation analyses, such as XRD, FTIR and SEM techniques. Various characteristics of the developed nanofluids from dispersing the synthesised NCs in distilled water, including pH, conductivity and density, have shown the reliability of these nanofluids. The minimum value of IFT was achieved for the crude oil–NF250 system, which was 22 mN/m, and the IFT was increased with increasing the concentration of the synthesised NCs. Additionally, by adding 250 ppm of the synthesised NC into distilled water, the wettability of the used carbonate rock was greatly altered from a strong oil-wet to a strong water-wet system, from 132.6 mN/m to 22° and 34.5°.

5 References

[1] Ali J.A., Kolo K., Khaksar Manshad A., *ET AL.*: 'Low-salinity polymeric nanofluid-enhanced oil recovery using green polymer-coated ZnO/SiO_2 nanocomposites in the upper Qamchuqa formation in Kurdistan region, Iraq', *Energy Fuels*, 2019, **33**, pp. 2927–2937, doi: 10.1021/acs.energyfuels.8b03847
[2] Ali J.A., Kalhury A.M., Sabir A.N., *ET AL.*: 'A state-of-the-art review of the application of nanotechnology in the oil and gas industry with a focus on drilling engineering', *J. Petrol Sci. Eng.*, 2020, **191**, pp. 107–118, doi: 10.1016/j.petrol.2020.107118
[3] Asl H.F., Zargar G., Manshad A.K., *ET AL.*: 'Effect of SiO_2 nanoparticles on the performance of L-Arg and L-Cys surfactants for enhanced oil recovery in carbonate porous media', *J. Mol. Liquids*, 2020, **300**, p. 112290
[4] Zargar G., Arabpour T., Khaksar Manshad A., *ET AL.*: 'Experimental investigation of the effect of green TiO_2/quartz nanocomposite on interfacial tension reduction, wettability alteration, and oil recovery improvement', *Fuel*, 2020, **263**, p. 116599

[5] Agista M., Guo K., Yu Z.: 'A state-of-the-art review of nanoparticles application in petroleum with a focus on enhanced oil recovery', *Appl. Sci.*, 2018, **8**, (6), pp. 871–880

[6] Sun X., Zhang Y., Chen G., *ET AL.*: 'Application of nanoparticles in enhanced oil recovery: a critical review of recent progress', *Energies*, 2017, **10**, (3), p. 345

[7] Almahfood M., Bai B.: 'The synergistic effects of nanoparticle-surfactant nanofluids in EOR applications', *J. Petrol. Sci. Eng.*, 2018, **171**, pp. 196–210

[8] Ershadi M., Alaei M., Rashidi A., *ET AL.*: 'Carbonate and sandstone reservoirs wettability improvement without using surfactants for chemical enhanced oil recovery (C-EOR)', *Fuel*, 2015, **153**, pp. 408–415

[9] Sagala F., Montoya T., Hethnawi A., *ET AL.*: 'Nanopyroxene-based nanofluids for enhanced oil recovery in sandstone cores at reservoir temperature', *Energy Fuels*, 2019, **33**, pp. 2877–2890

[10] Ali J.A., Kolo K., Manshad A.K., *ET AL.*: 'Recent advances in application of nanotechnology in chemical enhanced oil recovery: effects of nanoparticles on wettability alteration, interfacial tension reduction, and flooding', *Egyptian J. Petrol.*, 2018, **27**, (4), pp. 1371–1383

[11] Ahmadi M.A., Sheng J.: 'Performance improvement of ionic surfactant flooding in carbonate rock samples by use of nanoparticles', *Petrol. Sci.*, 2016, **13**, (4), pp. 725–736

[12] Sheng J.J.: 'Modern chemical enhanced oil recovery: theory and practice' (Gulf Professional Publishing, Houston, Texas, USA, 2010)

[13] Zhang H., Ramakrishnan T.S., Nikolov A., *ET AL.*: 'Enhanced oil recovery driven by nanofilm structural disjoining pressure: flooding experiments and microvisualization', *Energy Fuels*, 2016, **30**, (4), pp. 2771–2779

[14] Sharma T., Sangwai J.S.: 'Silica nanofluids in polyacrylamide with and without surfactant: viscosity, surface tension, and interfacial tension with liquid paraffin', *J. Petrol. Sci. Eng.*, 2017, **152**, pp. 575–585

[15] Ehtesabi H., Ahadian M.M., Taghikhani V., *ET AL.*: 'Enhanced heavy oil recovery in sandstone cores using TiO_2 nanofluids', *Energy Fuels*, 2013, **28**, (1), pp. 423–430

[16] Hendraningrat L., Torsaeter O.: 'Metal oxide-based nanoparticles: revealing their potential to enhance oil recovery in different wettability systems', *Appl. Nanosci.*, 2014, **5**, (2), pp. 181–199

[17] Ju B., Fan T.: 'Experimental study and mathematical model of nanoparticle transport in porous media', *Powder Technol.*, 2009, **192**, pp. 195–202

[18] Rezvani H., Riazi M., Tabaei M., *ET AL.*: 'Experimental investigation of interfacial properties in the EOR mechanisms by the novel synthesized Fe_3O_4@chitosan nanocomposites', *Colloids Surf. A, Physicochem. Eng. Aspects*, 2018, **544**, pp. 15–27

[19] Qi L., Song C., Wang T., *ET AL.*: 'Polymer-coated nanoparticles for reversible emulsification and recovery of heavy oil', *Langmuir*, 2018, **34**, pp. 6522–6528

[20] Lim S., Wasan D.: 'Structural disjoining pressure induced solid particle removal from solid substrates using nanofluids', *J. Colloid Interface Sci.*, 2016, **500**, pp. 96–104

[21] Ali J.A., Kolo K., Manshad A.K., *ET AL.*: 'Potential application of low-salinity polymeric-nanofluid in carbonate oil reservoirs: IFT reduction, wettability alteration, rheology and emulsification characteristics', *J. Mol. Liquids*, 2019, **284**, pp. 735–747

[22] Ali J.A., Kolo K., Sajadi S.M., *ET AL.*: 'Modification of rheological and filtration characteristics of water-based mud for drilling oil and gas wells using green SiO_2@ZnO@Xanthan nanocomposite', *IET Nanobiotechnol.*, 2019, **13**, (7), pp. 748–755, doi: 10.1049/iet-nbt.2018.5205

[23] Ali J.A., Manshad A.K., Imani I., *ET AL.*: 'Greenly synthesized magnetite@SiO_2@SiO_2@Xanthan nanocomposites and its application in enhanced oil recovery: IFT reduction and wettability alteration', *Arabian J. Sci. Eng.*, 2020, doi: 10.1007/s13369-020-04405-w

[24] Bahraminejad H., Khaksar Manshad A., Riazi M., *ET AL.*: 'Cuo/TiO_2/PAM as a novel introduced hybrid agent for water–oil interfacial tension and wettability optimization in chemical enhanced oil recovery', *Energy Fuels*, 2019, **33**, (11), pp. 10547–10560, doi: 10.1021/acs.energyfuels.9b02109

[25] Madhavi V., Prasad T.N.V.K.V., Reddy A.V. B., *ET AL.*: 'Application of phytogenic zerovalent iron nanoparticles in the adsorption of hexavalent chromium', *Spectrochim. Acta A, Mol. Biomol. Spectrosc.*, 2013, **116**, pp. 17–25

[26] Kuang Y., Wang Q., Chen Z., *ET AL.*: 'Heterogeneous Fenton-like oxidation of monochlorobenzene using green synthesis of iron nanoparticles', *J. Colloid Interface Sci.*, 2013, **410**, pp. 67–73

[27] Muthukumar H., Matheswaran M.: '*Amaranthus spinosus* leaf extract mediated FeO nanoparticles: physicochemical traits, photocatalytic and antioxidant activity', *ACS Sustain. Chem. Eng.*, 2015, **3**, (12), pp. 3149–3156, doi: 10.1021/acssuschemeng.5b00722

[28] Sajadi S.M., Nasrollahzadeh M., Maham M., *ET AL.*: 'Aqueous extract from seeds of *Silybum marianum* L. as a green material for preparation of the Cu/Fe_3O_4 nanoparticles: a magnetically recoverable and reusable catalyst for the reduction of nitroarenes', *J. Colloid Interface Sci.*, 2016, **469**, pp. 93–98

[29] Groiss S., Selvaraj R., Varadavenkatesan T., *ET AL.*: 'Structural characterization, antibacterial and catalytic effect of iron oxide nanoparticles synthesised using the leaf extract of *Cynometra ramiflora*', *J Mol. Struct.*, 2016, **1128**, pp. 572–578

[30] Sajadi M., Nasrollahzadeh M., Mohammad Sajadi S.: 'Green synthesis of Ag/Fe_3O_4 nanocomposite using *Euphorbia peplus* Linn leaf extract and evaluation of its catalytic activity', *J. Colloid Interface Sci.*, 2017, **497**, pp. 1–13

[31] Wei Y., Fang Z., Zheng L., *ET AL.*: 'Biosynthesized iron nanoparticles in aqueous extracts of *Eichhornia crassipes* and its mechanism in the hexavalent chromium removal', *Appl. Surf. Sci*, 2017, **399**, pp. 322–329

[32] Chen C.-C., Huang Y.-L., Ou J.-C., *ET AL.*: 'Three new prenylflavones from *Artocarpus altilis*', *J. Natural Products*, 1993, **56**, (9), pp. 1594–1597

[33] Sundarrao K., Burrows I., Kuduk M., *ET AL.*: 'Preliminary screening of antibacterial and antitumor activities of Papua new Guinean native medicinal plants', *Int. J. Pharmacognosy*, 1993, **31**, (1), pp. 3–6, doi: 10.3109/13880209309082909

[34] Sajadi S.M., Kolo K., Pirouei M., *ET AL.*: 'Natural iron ore as a novel substrate for the biosynthesis of bioactive-stable ZnO@CuO@iron ore NCs: a magnetically recyclable and reusable superior nanocatalyst for the degradation of organic dyes, reduction of Cr(vi) and adsorption of crude oil aromatic compounds, including PAHs', *RSC Adv.*, 2018, **8**, (62), pp. 35557–35570

[35] Han S.T.: 'Medicinal plants in south pacific' (World health organization, WHO regional publication, western pacific series.No.19, United States of America, 1998), pp. 9–10

[36] Fovet Y., Gal J.Y., Toumelin-Chemla F. 'Influence of pH and fluoride concentration on titanium passivating layer: stability of titanium dioxide', *Talanta*, 2001, **53**, pp. 1053–1063

[37] Wen D., Lin G., Vafaei S., *ET AL.*: 'Review of nanofluids for heat transfer applications', *Particuology*, 2009, **7**, pp. 141–150

[38] Kamal M.S., Hussein I.A., Sultan A.S.: 'Review on surfactant flooding: phase behavior, retention, IFT, and field applications', *Energy Fuels*, 2017, **31**, (8), pp. 7701–7720

[39] Eshraghi E.S., Kazemzadeh Y., Qahramanpour M., *ET AL.*: 'Investigating effect of SiO_2 nanoparticle and sodium-dodecyl-sulfate surfactant on surface properties: wettability alteration and IFT reduction', *J. Petrol. Environ. Biotechnol.*, 2017, **8**, (6), pp. 1–5, doi: 10.4172/2157-7463.100034

[40] Ali J.A., Kolo K., Khaksar Manshad A., *ET AL.*: 'Modification of LoSal water performance in reducing interfacial tension using green ZnO/SiO_2 nanocomposite coated by xanthan', *Appl. Nanosci.*, 2018, **9**, (3), pp. 397–409

[41] Ali J.A., Kolo K., Mohammed Sajad S., *ET AL.*: 'Green synthesis of ZnO/SiO_2 nanocomposite from pomegranate seed extract: coating by natural xanthan polymer and its characterisations', *Micro Nano Lett.*, 2019, **14**, (6), pp. 638–641, doi: 10.1049/mnl.2018.561

[42] Roustaei A., Moghadasi J., Bagherzadeh H., *ET AL.*: 'An experimental investigation of polysilicon nanoparticles' recovery efficiencies through changes in interfacial tension and wettability alteration'. SPE Int. Oilfield Nanotechnology Conf. and Exhibition; Society of Pet. Engineers, Noordwijk, The Netherlands, 2012, doi: 10.2118/156976-ms

[43] Joonaki E., Ghanaatian S.: 'The application of nanofluids for enhanced oil recovery: effects on interfacial tension and coreflooding process', *Pet. Sci. Technol.*, 2014, **32**, (21), pp. 2599–2607

[44] Esfandyari Bayat A., Junin R., Samsuri A., *ET AL.*: 'Impact of metal oxide nanoparticles on enhanced oil recovery from limestone media at several temperatures', *Energy Fuels*, 2014, **28**, (10), pp. 6255–6266

[45] Li Y., Dai C., Zhou H., *ET AL.*: 'Investigation of spontaneous imbibition by using a surfactant-free active silica water-based nanofluid for enhanced oil recovery', *Energy Fuels*, 2017, **32**, (1), pp. 287–293

[46] Soleimani H., Baig M.K., Yahya N., *ET AL.*: 'Synthesis of ZnO nanoparticles for oil–water interfacial tension reduction in enhanced oil recovery', *Appl. Phys. A*, 2018, **124**, (2), pp. 128–140

[47] Haroun M.R., Alhassan S., Ansari A.A., *ET AL.*: 'Smart nano-EOR process for Abu Dhabi carbonate reservoirs'. Proc. of the Abu Dhabi Int. Petroleum Conf. and Exhibition, Abu Dhabi, UAE, 11–14 November 2012